Math. Appl. 14(2)2025, 163–176

A NEW APPROACH TO MODELLING OF ZIKA VIRUS DISSEMINATION BY VECTOR USING GRAPH THEORY

P. Renisa[1], S. Sujitha[2*], and M. K. Angel Jebitha[3]

Abstract: *The Zika virus (ZIKV), a mosquito-borne pathogen, has emerged as a major global health concern due to its link with congenital abnormalities and neurological disorders. This paper introduces a novel graph-theoretic framework for modelling ZIKV transmission through its primary vector, Aedes mosquitoes. In this approach, epidemiological compartments of the transmission cycle are represented as nodes, while transitions between human and mosquito states are modelled as edges. The adjacency matrix derived from this graph enables the computation of eigenvalues, from which the graph-theoretic basic reproduction number (RN) is defined through the energy and iota energy of the digraph. Unlike traditional compartmental models, the graph-based method provides a structural perspective on the interplay between human and vector dynamics. The model was applied to reported Zika cases in Brazil (2015–2016 outbreak), and further illustrated using infection fractions and population data from Yap, Moorea, Tahiti, and New Caledonia. The results demonstrate that RN exceeds unity when infection levels are sufficiently high, while remaining below threshold under lower prevalence conditions. This indicates that the proposed framework captures epidemic threshold behaviour and offers a flexible tool for analyzing region-specific outbreak scenarios.*

Introduction

The Zika virus, a member of the Spondweni serocomplex of the genus Flavivirus in the family Flaviviridae, has emerged as a prominent global health concern in recent years [17]. Characterized by mild symptoms in most cases, its sudden resurgence in the early 21st century raised alarms due to its association with severe defects in newborn infants and with neurological and auto-immune disorders such as microcephaly [8], [16].
Two species of mosquitoes were identified as the main vectors for ZIKV transmission, namely Aedes aegypti and Aedes albopictus. They seem to have different habitats, geographical distribution, feeding preference and susceptibilities to ZIKV [15]. These mosquitoes are widespread in many tropical and subtropical regions, making the virus a potential threat to a large population. Before 2007, human cases of Zika were rare and sporadic in Africa and Asia for many years with mild or no symptoms reported. In 2007,

[1]Research Scholar (Reg. No. 21213042092003), Department of Mathematics, Holy Cross College (Autonomous), Nagercoil-629004, affiliated to Manonmaniam Sundaranar University, Abishekapatti, Tirunelveli-627012, India. Email: renisa98pandian@gmail.com
[2]Assistant Professor, Department of Mathematics, Holy Cross College (Autonomous), Nagercoil-629004, India. *Corresponding author. Email: sujitha.s@holycrossngl.edu.in
[3]Assistant Professor, Department of Mathematics, Holy Cross College (Autonomous), Nagercoil-629004, India. Email: angeljebitha@holycrossngl.edu.in

Keywords: Zika virus, adjacency matrix, graph-theoretic basic reproduction number, graph energy, iota energy, mosquito biting rate, vector transmission, numerical data, simulation analysis, eigenvalues.
AMS Subject Classification: 05C20, 05C22, 47A10, 00A71.

the first outbreak in the Pacific occurred in Yap, followed in 2013 by a large outbreak in French Polynesia, leading to a sharp increase in reported cases. Then, it rapidly spread throughout the Americas, with outbreaks in Brazil, Colombia and other countries. One of the most affected countries in the world is Brazil [18]. The number of suspected cases in Brazil was estimated at 440,000 to 1,300,000 in 2015. The link between Zika infection during pregnancy and microcephaly in newborns was established, causing widespread concern. The World Health Organization (WHO) declared Zika a public health emergency in February 2016.

Many researchers are constructing mathematical models for Zika virus transmission to investigate the effect of its outbreak using various parameters and various factors of transmission. Suparit et al. presented a mathematical model for Zika virus to investigate the transmission dynamics with a time-dependent mosquito biting rate [18]. Agusto et al. analyzed a ZIKV model that includes human vertical transmission, birth of babies with microcephaly and asymptomatic infected individuals [1]. Chitnis et al. described a compartmental model for malaria transmission to determine the relative importance of model parameters to disease transmission and prevalence [7]. Heffernan et al. studied the concept of the basic reproductive ratio, which is fundamental to the study of epidemiology and within-host pathogen dynamics [11]. Barve et al. presented a mathematical model to observe the effect of sexual transmission on gender and symptoms based division of the infected human population [3]. Early researchers have calculated the basic reproduction number (R_0) using differential equations upon the compartmental models of Zika virus transmission.

Graphical modelling offers a powerful framework for representing and analyzing complex systems, making them particularly well-suited for deciphering the multifaceted nature of infectious diseases. In this context, the graphical model serves as a versatile tool for visualizing and quantifying the relationships between various factors influencing Zika transmission, including vector populations, environmental factors, human mobility and genetic variations in the virus. This method utilizes graph theory to model transmission dynamics, with nodes representing SEIR compartments and edges indicating potential pathways of disease spread.

Graph theory is a branch of mathematics that studies the relationships between objects represented as vertices or nodes, connected by edges or arcs. Graphs can be used to model and analyze a wide range of real-world phenomena. Adjacency matrices can help model the spread of Zika virus by showing how it moves between different groups of people and mosquitoes. The eigenvalues of the associated matrices and its energy provide insight into the stability and resilience of the network. Additionally, the graph-theoretic basic reproduction number (R_N), a crucial epidemiological index, can be defined by analyzing the energy and iota energy of the transmission digraph. The model parameters span a range influenced by real-world data, including vector-host interactions, environmental factors, and intervention measures.

The present work aims to approach the compartmental model of Zika virus dissemination by vector using graph theory [6]. The graph is derived using the SEIR compartmental model. One of the most popular modelling frameworks is the compartmental model, in which the population is divided

into four compartments, namely Susceptible (S), Exposed (E), Infectious (I) and Recovered (R). This compartmental model has been employed in the study of transmission dynamics in many vector-borne diseases such as Zika virus, Dengue, Chikungunya and Malaria. The present model is a modification of the model discussed by Suparit et al. The H and V subscripts in the variables denote human and vector populations, respectively. The human population follows an SEIR compartmental model and the vector population follows an SEI compartmental model. The total human population (N_H) consists of four mutually exclusive compartments, which are as follows:

1. Susceptible human (S_H)
2. Exposed human (E_H)
3. Infectious human (I_H)
4. Recovered human (R_H)

The total vector population is divided into three compartments, namely Susceptible, Exposed and Infectious vectors, denoted by S_V , E_V and I_V respectively. The human population size (N_H) is constant, that is, $S_H + E_H + I_H + R_H = N_H$. Some of the basic definitions used in this study are as follows.

Definition 1. A *digraph* $D = (V, E)$ consists of a finite nonempty set V of objects called *vertices* and a set E of ordered pairs of distinct vertices. Each element of E is an *arc* or a *directed edge* [6].

Definition 2. A *weighted digraph* $D = (V, E, w)$ is a digraph in which each edge is assigned a number, called a weight.

Definition 3. Suppose $A_{n\times n}$ is a square matrix. Then $A - \lambda I$ is called the *eigen* or *characteristic matrix*, where λ is an indefinite scalar and I is the identity matrix. The determinant $|A - \lambda I|$ is the characteristic polynomial and $|A - \lambda I| = 0$ is the *eigen equation* or *characteristic equation*. The roots of the characteristic equation are called *eigenvalues* [13].

The remainder of this paper is organized as follows. The second section presents the derivation of the graphical model, where the human population is divided into four classes and the vector population into three classes. All vertices (representing compartments) and edges (representing transmission parameters) are defined, and the corresponding adjacency matrix of the derived graph is determined. The third section introduces the computation of graph energy, specifies the range of model parameters, and defines the graph-theoretic basic reproduction number (R_N) from the model. The fourth section presents the main theoretical results and analyzes the epidemiological dynamics by applying the model to secondary data from the 2015–2016 Zika virus outbreak in Brazil. The fifth section extends the numerical analysis to country-specific infection fractions and population data from Yap, Moorea, Tahiti, and New Caledonia. Finally, the sixth section concludes the study with a summary of key findings and their implications for understanding Zika virus transmission dynamics.

Graphical Model and Adjacency Matrix

Graphical modelling helps to understand complex systems by representing them as graphs. When studying the spread of the Zika virus, we can convert real-world data into a graph to visualize how the virus spreads between

individuals, regions, and mosquito populations. In this section, we discuss how the Zika virus transmission model can be converted into a graph, highlighting its structure, nodes and edges, and showing key components like infected individuals, mosquitoes, and transmission routes. The digraph D consists of vertices V and edges E, written as $D = (V, E)$, where

$$V(D) = \{v_1, v_2, v_3, v_4, v_5, v_6, v_7\},$$

$$E(D) = \{v_1v_2,\ v_2v_3,\ v_3v_4,\ v_3v_5,\ v_7v_1,\ v_5v_6,\ v_6v_7\}.$$

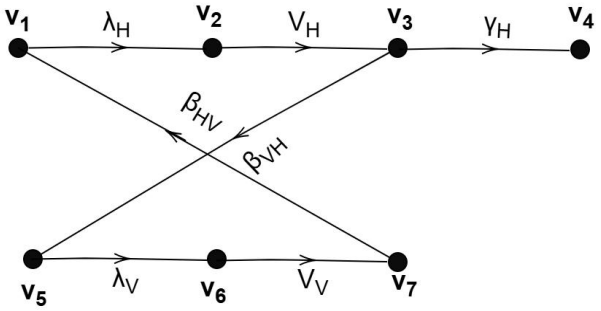

Figure 1: Schematic of the Zika transmission graphical model.

In Figure 1, the above-mentioned seven compartments are chosen as the vertices. The edges of the graph are defined if there occurs a rate of transmission between the vertices. Susceptible humans (S_H) can be infected if they are bitten by infectious mosquitoes. Then the infected humans immediately become exposed (E_H) and enter the infectious class (I_H) after the intrinsic incubation period. Finally, infectious humans move to the recovered class (R_H). Susceptible mosquitoes (S_V) become exposed (E_V) when they bite infectious humans and then they become infectious (I_V). Therefore, the edge set is

$$E(D) = \{v_1v_2, v_2v_3, v_3v_4, v_3v_5, v_7v_1, v_5v_6, v_6v_7\}.$$

The remaining possible directed edges would contradict the natural flow of disease progression and are therefore not valid in the model. Each state follows a specific order, and reversing or skipping transitions would misrepresent the real-world dynamics of infection. The weights assigned to the edges of the graph are determined based on key parameters that define the transmission dynamics of the Zika virus. These parameters include factors such as the infection rate, transmission probability between hosts and vectors, infectious period, and recovery rate. The edge weight represents the likelihood or intensity of transition between states.
The weight set of the derived graph is

$$w(D) = \{\lambda_H, v_H, \gamma_H, \beta_{VH}, \beta_{HV}, \lambda_V, v_V\},$$

where λ_H is the force of infection of susceptible humans from an infectious mosquito; v_H is the human progression rate from the exposed state to the infectious state; γ_H is the human recovery rate; β_{VH} is the probability of pathogen transmission from an infectious human to a susceptible mosquito; β_{HV} is the probability of pathogen transmission from an infectious

mosquito to a susceptible human; λ_V is the force of infection of susceptible vectors from an infectious human when they bite; and v_V is the mosquito progression rate from the exposed state to the infectious state.

Adjacency Matrix

In Zika virus modelling, an adjacency matrix is used to represent the network of interactions between different factors, such as human populations, mosquito populations, and the virus itself. It is a way to visualize and understand how these entities are connected and how the virus spreads through the network. Since the graph-theoretic basic reproduction number R_N is proportional to $P^{1/6}$ (see Theorem 1), where P is the product of the edge weights, each weight parameter (e.g., infection rate, transmission probability, progression rate) influences R_N with the same elasticity $1/6$; the effect of varying the biting rates and infected fractions is examined in the fourth and fifth sections.

Definition 4. The adjacency matrix $A(D) = [a_{ij}]_{n\times n}$ of an n-vertex weighted digraph D is defined as

$$a_{ij} = \begin{cases} w(v_i, v_j), & \text{if there is an edge from } v_i \text{ to } v_j, \\ 0, & \text{otherwise.} \end{cases}$$

Figure 1 represents a weighted directed graph (digraph) $D = (V, E)$. Therefore the adjacency matrix of D is

$$A(D) = \begin{pmatrix} 0 & \lambda_H & 0 & 0 & 0 & 0 & 0 \\ 0 & 0 & v_H & 0 & 0 & 0 & 0 \\ 0 & 0 & 0 & \gamma_H & \beta_{VH} & 0 & 0 \\ 0 & 0 & 0 & 0 & 0 & 0 & 0 \\ 0 & 0 & 0 & 0 & 0 & \lambda_V & 0 \\ 0 & 0 & 0 & 0 & 0 & 0 & v_V \\ \beta_{HV} & 0 & 0 & 0 & 0 & 0 & 0 \end{pmatrix}.$$

The characteristic equation of this matrix is $(-\lambda)(\lambda^6 - P) = 0$, where $P = \lambda_H v_H \beta_{VH} \lambda_V v_V \beta_{HV}$. Therefore, the seven roots are $\lambda_1 = 0$ and the six roots of $\lambda^6 - P = 0$, given by

$$\lambda_{k+2} = P^{1/6}\left(\cos\frac{\pi k}{3} + i\sin\frac{\pi k}{3}\right), \qquad 0 \le k \le 5.$$

That is, the six roots are $P^{1/6}$ multiplied by the six 6th roots of unity $1, -1, 1/2 + i\sqrt{3}/2$, $-1/2 + i\sqrt{3}/2$, $1/2 - i\sqrt{3}/2$ and $-1/2 - i\sqrt{3}/2$, which implies $\pm 1, \pm 0.5 \pm 0.866i$.

Energy, Graph-theoretic Basic Reproduction Number and Range of the Model Parameters

Energy of a Digraph

In 1978, Gutman [9] introduced the concept of energy of a simple graph. He defined the energy of a graph as the sum of the absolute values of its eigenvalues. Since the adjacency matrix of a digraph is not necessarily symmetric, its eigenvalues may be complex. The energy of a digraph is defined as the sum of the absolute values of the real parts of its eigenvalues. Khan et al. [14] introduced the notion of iota energy of digraphs as the sum of the absolute values of the imaginary parts of its eigenvalues. Hafeez and Khan [10] extended the concept of iota energy to weighted digraphs, and this iota energy plays a major role in finding the graph-theoretic basic reproduction number in this study.

Definition 5. Let D be a weighted digraph with eigenvalues $\lambda_1, \lambda_2, \ldots, \lambda_n$. Then the energy of D is [4]

$$\mathcal{E}(D) = \sum_{k=1}^{n} |\mathrm{Re}(\lambda_k)|,$$

where $\mathrm{Re}(\lambda_k)$ denotes the real part of the eigenvalue λ_k.

Definition 6. Let D be a weighted digraph with eigenvalues $\lambda_1, \lambda_2, \ldots, \lambda_n$. Then the iota energy of D is [10]

$$\mathcal{E}_c(D) = \sum_{k=1}^{n} |\mathrm{Im}(\lambda_k)|,$$

where $\mathrm{Im}(\lambda_k)$ denotes the imaginary part of the eigenvalue λ_k.

Graph-theoretic Basic Reproduction Number

In epidemiology, understanding the transmission dynamics of infectious diseases is paramount for effective disease control and public health interventions. Central to this understanding is the concept of the basic reproduction number, denoted R_0 [11], [12]. The basic reproduction number serves as a key metric in assessing the transmissibility of infectious diseases within populations.

Definition 7. The *classical basic reproduction number* R_0 is defined as the number of new infections produced by one infected individual in a completely susceptible population. It is a function of the baseline parameters.

Definition 8. The *graph-theoretic basic reproduction number* of a weighted digraph D with eigenvalues $\lambda_1, \ldots, \lambda_n$, denoted by R_N, is defined by

$$R_N = \mathcal{E}(D) + 2\,\mathcal{E}_c(D) = \sum_{k=1}^{n} |\mathrm{Re}(\lambda_k)| + 2\sum_{k=1}^{n} |\mathrm{Im}(\lambda_k)|.$$

After calculating the adjacency matrix, the corresponding eigenvalues are calculated using the characteristic equation and R_N is obtained from them using the formula of Definition 8. R_N is a structural index computed from the spectrum of the transmission digraph; it is not obtained from the next-

generation matrix and is therefore distinguished from the classical R_0. The weight 2 on the iota energy is a modelling choice that gives the imaginary (cyclic) part of the spectrum, which reflects the closed human–vector–human transmission loop, greater emphasis than the real part. Calibrating this weight against classical R_0 estimates is left for future work. Moreover, since the forces of infection depend on the infected fractions, R_N is a prevalence-conditioned index and, unlike R_0, it is not evaluated in a completely susceptible population.

We adopt $R_N = 1$ as the working epidemic threshold. If $R_N < 1$, transmission is not sustained and the disease will likely die out in the population over time as the number of infected individuals decreases. If $R_N = 1$, the system is at the critical case; the disease may persist in the population (endemic equilibrium), but it will neither grow nor decline. If $R_N > 1$, the disease is likely to spread within the population, leading to an epidemic if not controlled.

Theorem 1. For the digraph D of Figure 1, $R_N = 4\left(1+\sqrt{3}\right)P^{1/6} \approx 10.928\,P^{1/6}$, where $P = \lambda_H v_H \beta_{VH} \lambda_V v_V \beta_{HV}$.

Proof. The eigenvalues are 0 and $\rho\, e^{i\pi k/3}$, $k = 0,1,\ldots,5$, where $\rho = P^{1/6}$. Then

$$\sum|\mathrm{Re}(\lambda_k)| = \rho(1+1+4\cdot 1/2) = 4\rho$$
$$\sum|\mathrm{Im}(\lambda_k)| = 4\cdot\sqrt{3}/2\,\rho = 2\sqrt{3}\,\rho.$$

Hence

$$R_N = 4\rho + 2\left(2\sqrt{3}\,\rho\right) = 4\left(1+\sqrt{3}\right)\rho.$$

▫

Remark 1. If λ_H and λ_V are proportional to the infected fraction p, then $P \propto p^2$ and $R_N \propto p^{1/3}$, so R_N increases monotonically with p. The threshold $R_N = 1$ corresponds to $P = \left[4\left(1+\sqrt{3}\right)\right]^{-6} \approx 5.87 \times 10^{-7}$.

Remark 2. Vertex v_4 (recovered humans) is a terminal vertex, so the recovery weight γ_H does not appear in the characteristic polynomial. Consequently R_N is independent of the human infectious period; this is a structural limitation of the present digraph.

Range of the Parameters

In the simulations, the ranges of the parameters are described in Table 1. Most of the parameter values used in this study were derived from, or extensively referenced in, Manore et al. [15], who provided an inclusive sensitivity analysis of how the predictions of the model change with variations in the key parameters. To support the assessment of uncertainty in the parameters, we scrutinize the behaviour of the model over a wide range of feasible parameters.

Table 1. Descriptions and ranges of all the parameters used in this model.

Parameter	Description	Range	Reference
σ_H	Maximum number of bites a human can sustain	1 – 50	[15]
σ_V	Mosquito biting rate	0.01 – 0.35	[18]
β_{HV}	Probability of pathogen transmission from an infectious mosquito to a susceptible human	0.1 – 0.75	[7]
β_{VH}	Probability of pathogen transmission from an infectious human to a susceptible mosquito	0.1 – 0.75	[7]
$1/v_H$	Intrinsic incubation period (days)	3 – 14	[2]
$1/v_V$	Extrinsic incubation period (days)	8 – 12	[2]
$1/\gamma_H$	Human infectious period (days)	4 – 12	[15]
N_V	Mosquito population size	10 – 250 million	[18]
N_H	Human population size considered for Brazil	15,276,566	[18]

The force of infection for humans (λ_H) and the force of infection for mosquitoes (λ_V) are the rates at which infectious individuals infect others [18]:

$$\lambda_H = \frac{\sigma_V \sigma_H N_V}{\sigma_V N_V + \sigma_H N_H} \beta_{HV} \frac{I_V}{N_V},$$

$$\lambda_V = \frac{\sigma_V \sigma_H N_H}{\sigma_V N_V + \sigma_H N_H} \beta_{VH} \frac{I_H}{N_H}.$$

We also need to assume the values of I_V/N_V (proportion of infectious mosquitoes) and I_H/N_H (proportion of infectious humans). According to the total population of humans and mosquitoes chosen from the given sample, let us assume that the proportion of infected humans and mosquitoes is 0.001 (1 in 1000 individuals). We analyze the force of infection of humans and mosquitoes and also the graph-theoretic basic reproduction number by taking 1 in 1000 individuals as infected. Here $N_H = 15{,}276{,}566$ is the study population adopted in this work (cf. [18]) and it is smaller than the national population of Brazil, so the results are region-specific. For this low-prevalence illustration we take $N_V = 10^7$ (the lower end of the range in Table 1). In Table 1, the transmission probabilities β_{HV}, β_{VH} are used at the baseline value 0.1 inside λ_H, λ_V, whereas the edge weights β_{VH}, β_{HV} in P are varied over 0.1–0.75 to obtain the lower and upper bounds of R_N ; this convention is followed throughout the fourth and fifth sections. Using the ranges of the parameters listed in Table 1, we discuss the following results.

Main Results

Theorem 2. If $\sigma_H = 1$, $0.01 \le \sigma_V \le 0.35$, $\beta_{HV} = \beta_{VH} = 0.1$, $I_V/N_V = I_H/N_H = 0.001$ and $N_V = 10^7$, then the forces of infection for humans (λ_H) and mosquitoes (λ_V) satisfy $6.5 \times 10^{-7} \le \lambda_H \le 1.86 \times 10^{-5}$ and $9.9 \times 10^{-7} \le \lambda_V \le 2.85 \times 10^{-5}$, respectively. Equivalently, $\lambda_H = c_H \sigma_V \beta_{HV}$ and $\lambda_V = c_V \sigma_V \beta_{VH}$, where c_H decreases from 6.5×10^{-4} to 5.286×10^{-4} and c_V decreases from 9.9×10^{-4} to 8.143×10^{-4} as σ_V increases from 0.01 to 0.35.

Proof. **Case (i).** We know that

$$\lambda_H = \frac{\sigma_V \sigma_H N_V}{\sigma_V N_V + \sigma_H N_H} \beta_{HV} \frac{I_V}{N_V}.$$

Substituting the values of σ_H, β_{HV}, I_V/N_V, N_V and N_H, we get

$$\lambda_H = \frac{\sigma_V \times 1 \times 10^7}{\sigma_V \times 10^7 + 1 \times 15276566} \times 0.0001.$$

Now we compute the bounds of λ_H by substituting the lower and upper bounds of σ_V.

Subcase (i). For $\sigma_V = 0.01$,

$$\lambda_H = \frac{0.01 \times 1 \times 10^7}{0.01 \times 10^7 + 1 \times 15276566} \times 0.0001 = 0.00000065,$$

which is approximately $0.00065 \times 0.01 \times 0.1$, that is, $6.5 \times 10^{-4}\sigma_V\beta_{HV}$.

Subcase (ii). For $\sigma_V = 0.35$,

$$\lambda_H = \frac{0.35 \times 1 \times 10^7}{0.35 \times 10^7 + 1 \times 15276566} \times 0.0001 = 0.0000186,$$

which is approximately $0.0005286 \times 0.35 \times 0.1$, that is, $5.286 \times 10^{-4}\sigma_V\beta_{HV}$.

Case (ii). We know that

$$\lambda_V = \frac{\sigma_V\sigma_H N_H}{\sigma_V N_V + \sigma_H N_H}\,\beta_{VH}\,\frac{I_H}{N_H}.$$

Substituting the values of σ_H, β_{VH}, I_H/N_H, N_V and N_H, we get

$$\lambda_V = \frac{\sigma_V \times 1 \times 15276566}{\sigma_V \times 10^7 + 1 \times 15276566} \times 0.0001.$$

Now we compute the bounds of λ_V.

Subcase (i). For $\sigma_V = 0.01$,

$$\lambda_V = \frac{0.01 \times 1 \times 15276566}{0.01 \times 10^7 + 1 \times 15276566} \times 0.0001 = 0.000001,$$

which is approximately $0.00099 \times 0.01 \times 0.1$, that is, $9.9 \times 10^{-4}\sigma_V\beta_{VH}$.

Subcase (ii). For $\sigma_V = 0.35$,

$$\lambda_V = \frac{0.35 \times 1 \times 15276566}{0.35 \times 10^7 + 1 \times 15276566} \times 0.0001 = 0.0000285,$$

which is approximately $0.0008143 \times 0.35 \times 0.1$, that is, $8.143 \times 10^{-4}\sigma_V\beta_{VH}$.

Since λ_H and λ_V are increasing in σ_V, the numerical bounds stated in the theorem follow. These bounds on λ_H and λ_V inform the evaluation of the graph-theoretic basic reproduction number R_N for epidemiological insight.

Observation 1. For $0.01 \le \sigma_V \le 0.35$ and $1 \le \sigma_H \le 50$, the lower bounds of λ_H and λ_V are 0.00000065 and 0.000001, respectively.

Observation 2. For $0.01 \le \sigma_V \le 0.35$ and $1 \le \sigma_H \le 50$, the upper bounds of λ_H and λ_V are given in Table 2.

Table 2. Force of infection (upper bounds).

σ_H	Upper bound of λ_H	σ_H	Upper bound of λ_V
1	0.0000186	1	0.0000285
2	0.0000206	2	0.0000314
3	0.0000213	3	0.0000325
4	0.0000217	4	0.0000331
5	0.0000219	5	0.0000335
6	0.0000221	6	0.0000337
7	0.0000222	7 to 10	0.0000339 to 0.0000342
8, 9	0.0000223	11, 12	0.0000343
10, 11	0.0000224	13, 14	0.0000344
12, 13, 14	0.0000225	15, 16, 17	0.0000345
15 to 19	0.0000226	18 to 22	0.0000346
20 to 32	0.0000227	23 to 31	0.0000347
33 to 50	0.0000228	32 to 50	0.0000348

Theorem 3. If $\sigma_H = 1$, $6.5 \times 10^{-7} \le \lambda_H \le 1.86 \times 10^{-5}$ and $1 \times 10^{-6} \le \lambda_V \le 2.85 \times 10^{-5}$, then the graph-theoretic basic reproduction number satisfies $R_N < 1$ for the given range of the remaining parameters in Table 1.

Proof. Given: $1/14 \le v_H \le 1/3$, $1/12 \le v_V \le 1/8$ and $0.1 \le \beta_{HV}, \beta_{VH} \le 0.75$. The characteristic polynomial of the derived matrix is $(-\lambda)\left(\lambda^6 - P\right) = 0$, where $P = \lambda_H v_H \beta_{VH} \lambda_V v_V \beta_{HV}$. Since P is increasing in each of its factors, $R_N = 4\left(1+\sqrt{3}\right)P^{1/6}$ is bracketed by its values at the lower and upper bounds of the parameters.

Case (i). Substituting all the lower bounds of the parameters, we get $(-\lambda)\left(\lambda^6 - 3.869 \times 10^{-17}\right) = 0$, and the corresponding eigenvalues are 0, ± 0.00184, $\pm 0.00092 \pm 0.00159i$. Therefore the graph-theoretic basic reproduction number is

$$R_N = \mathcal{E}(D) + 2\mathcal{E}_c(D) = 0.00736 + 0.01272 = 0.02008 < 1.$$

Case (ii). Substituting all the upper bounds of the parameters, we get $(-\lambda)\left(\lambda^6 - 1.24 \times 10^{-11}\right) = 0$, and the corresponding eigenvalues are 0, ± 0.0152, $\pm 0.0076 \pm 0.0132i$. Therefore

$$R_N = \sum|\mathrm{Re}(\lambda_k)| + 2\sum|\mathrm{Im}(\lambda_k)| = 0.16644,$$

which is less than 1 for the parameter range considered (with $\sigma_H = 1$), indicating that transmission is not sustained in the population. ▫

Theorem 4. For the maximum values of σ_H, λ_H and λ_V (with σ_H up to 50), the graph-theoretic basic reproduction number satisfies $R_N < 1$.

Proof. The maximum values of σ_H, λ_H and λ_V are 50, 0.0000228 and 0.0000348 (from Observations 1 and 2). Substituting all the upper bounds of the parameters (Table 1) to compute R_N, we get $P = 1.85 \times 10^{-11}$, so the characteristic equation is $(-\lambda)\left(\lambda^6 - 1.85 \times 10^{-11}\right) = 0$. The corresponding eigenvalues are 0, ± 0.01628, $\pm 0.00814 \pm 0.0141i$. Therefore $R_N = 0.17792$, which implies that transmission is not sustained ($R_N < 1$). ▫

If the proportion of infected humans and mosquitoes is assumed to be 0.001 (1 in 1000 individuals), then it does not lead to an epidemic condition, since the graph-theoretic basic reproduction number is always less than 1. Let us now take the human population size of Brazil and the number of Zika-infected people during the 2015–2016 outbreak in Brazil, i.e., 1.2081 million in 15,276,566, which gives the proportion 0.079. This ratio is the cumulative fraction infected during the outbreak rather than the instantaneous prevalence, so it is used here as an upper-level proxy for I_H/N_H . We assume the proportion of infected mosquitoes and humans as 0.079. The mosquito population size is assumed to be 50 million (a mosquito-to-human ratio $N_V/N_H \approx 3.3$), since the number of infected mosquitoes increases with the increase in the infected human population; this ratio is also used to scale the mosquito populations in the numerical analysis section.

Theorem 5. If $\sigma_H = 1$, $0.01 \le \sigma_V \le 0.35$, $\beta_{HV} = \beta_{VH} = 0.1$, $I_V/N_V = I_H/N_H = 0.079$ and $N_V = 5 \times 10^7$, then the bounds of λ_H and λ_V are $2.5 \times 10^{-4} \le \lambda_H \le 4.2 \times 10^{-3}$ and $7.7 \times 10^{-5} \le \lambda_V \le 1.3 \times 10^{-3}$, respectively.

Proof. The proof is similar to that of Theorem 2. ▫

Observation 3. For $0.01 \le \sigma_V \le 0.35$ and $1 \le \sigma_H \le 50$: (i) the lower bounds of λ_H and λ_V are 0.00025 and 0.000077, respectively; (ii) the upper bounds of λ_H and λ_V are 0.0089 and 0.0027, respectively.

Theorem 6. For the maximum values of σ_H, λ_H and λ_V, the graph-theoretic basic reproduction number satisfies $R_N < 1$.

Proof. The maximum values of σ_H, λ_H and λ_V are 50, 0.0089 and 0.0027 (from Observation 3). Substituting all the upper bounds of the parameters (Table 1) to find the energy and iota energy of D, and then R_N, we get

$$P = \lambda_H v_H \beta_{VH} \lambda_V v_V \beta_{HV}$$
$$= 0.0089 \times 0.0027 \times 0.75 \times 0.75 \times 0.3333 \times 0.125 = 5.63 \times 10^{-7},$$

so the resultant polynomial is $(-\lambda)\left(\lambda^6 - 5.63 \times 10^{-7}\right) = 0$. The corresponding eigenvalues are 0, ± 0.0909, $\pm 0.0454 \pm 0.0787i$. Therefore $R_N = 0.993$, which is less than 1 and implies that transmission is not sustained under this scenario. ▫

Remark 3. Although the graph-theoretic basic reproduction number is currently estimated as $R_N = 0.993$, it lies very close to the epidemic threshold of 1. This indicates that the value of R_N is near a critical point. A slight increase in transmission-related parameters or a growth in the infected population could push R_N beyond 1, potentially leading to sustained disease transmission and an outbreak. Hence, continuous monitoring and control interventions remain crucial even in the sub-threshold regime.

Numerical Analysis of Zika Transmission Across Countries

In this section, we present a numerical analysis of Zika virus transmission dynamics using population data from four island settings that experienced

major outbreaks: Yap, Moorea, Tahiti, and New Caledonia. These countries were selected because reliable epidemiological data, including population size and estimated proportion of infected individuals, are available from published studies. Instead of applying a single fixed proportion, we used country-specific infection fractions based on reported outbreak data: 74% for Yap, 50% for Moorea, 50% for Tahiti, and 40% for New Caledonia [5]. These fractions are cumulative attack rates rather than instantaneous prevalence, so the resulting values should be read as upper-level illustrations. The mosquito population size was scaled relative to the human population following the same ratio used in the Brazil reference case ($N_V/N_H \approx 3.27$). The forces of infection were evaluated with $\sigma_H = 50$, $\sigma_V = 0.35$ and

$$\beta_{HV} = \beta_{VH} = 0.1,$$

and the edge weights in P were taken at the upper values $v_H = 1/3$, $v_V = 1/8$ and

$$\beta_{VH} = \beta_{HV} = 0.75,$$

exactly as in the Brazil case. Because N_V/N_H is fixed, λ_H and λ_V depend only on the infection fraction, so settings with equal infection fractions (Moorea and Tahiti) have equal R_N; the population sizes only determine I_H. These values were then used in our graph-based modelling framework to calculate the graph-theoretic basic reproduction number (R_N) and to illustrate the behaviour of the derived formula across different epidemiological contexts. The resulting R_N for each chosen country is summarized in Table 3.

Table 3. Estimated infected populations, baseline forces of infection and R_N.

Country	Infection fraction	N_H	I_H	λ_H	λ_V	R_N
Brazil	0.079	15,276,566	1,208,100	0.0089	0.0027	0.993 < 1
Yap	0.74	6,892	5,100	0.08287	0.02532	2.092 > 1
Moorea	0.50	16,200	8,100	0.056	0.017	1.8346 > 1
Tahiti	0.50	178,000	89,000	0.056	0.017	1.8346 > 1
New Caledonia	0.40	268,767	107,507	0.045	0.014	1.7048 > 1

Table 3 shows notable variation in the transmission intensity of Zika virus across the selected countries. Although Brazil recorded the largest number of infected individuals because of its large population size, its infection fraction is comparatively low and the basic reproduction number remains below the epidemic threshold (R_N=0.993<1), indicating limited sustained transmission under baseline conditions. In contrast, Yap, Moorea, Tahiti, and New Caledonia all have R_N>1, confirming favorable conditions for continued spread of infection. Among them, Yap exhibits the highest infection fraction, largest human and vector forces of infection, and the highest reproduction number, indicating the strongest transmission potential. Thus, the results indicate that regions with higher transmission efficiency are more vulnerable to sustained outbreaks, even when the total population size is relatively small.

CONCLUSION

In the present paper, we analyzed a graphical model for Zika virus dissemination as an alternative to classical differential equation models. The model was formulated using graph theory, from which the adjacency matrix and corresponding eigenvalues were derived. Based on these eigenvalues, the energy and iota energy of the graph D were computed, leading to the definition of the graph-theoretic basic reproduction number

$$R_N = \mathcal{E}(D) + 2\,\mathcal{E}_c(D) = \sum_{k=1}^{n} |\mathrm{Re}(\lambda_k)| + 2\sum_{k=1}^{n} |\mathrm{Im}(\lambda_k)|,$$

which for the present digraph reduces to $R_N = 4\left(1+\sqrt{3}\right)P^{1/6}$.

Theoretical analysis across a range of parameter values showed that R_N increases with the proportion of infected individuals (in fact $R_N \propto p^{1/3}$), and exceeds 1 when infections are sufficiently widespread, implying epidemic potential. To further illustrate the method, numerical analysis was carried out using country-specific infection fractions and population data from four Pacific island outbreaks. For Yap, Moorea, Tahiti, and New Caledonia, the R_N values obtained from the graph-based method exceed 1, in line with the epidemic nature of these outbreaks. These results demonstrate that the proposed framework is capable of capturing threshold behaviour and transmission patterns using graph-theoretic principles. A limitation is that R_N does not depend on the recovery rate γ_H.

Overall, the study highlights that controlling the fraction of infected humans (and consequently infected mosquitoes) is critical to keeping $R_N < 1$, thereby preventing epidemic spread. As future work, the model can be refined by incorporating real-time, region-specific data to yield more precise epidemiological predictions and to support public health strategies for localized outbreak control.

References

[1] F. Agusto, S. Bewick, W. Fagan, *Mathematical model of Zika virus with vertical transmission*, Infectious Disease Modelling **2** (2017), 244–267.

[2] S. Bañuelos, M. V. Martinez, C. Mitchell, A. Prieto-Langarica, *Mathematical modelling to investigate the effect of the sexual behaviour of asymptomatic individuals and vector control measures on Zika*, Letters in Biomathematics **6** (2019), 1–19.

[3] T. Barve, S. K. Tiwari, P. Porwal, *A mathematical model for the sexual transmission of Zika virus based on gender and symptoms*, South East Asian Journal of Mathematics and Mathematical Sciences **18** (2022), 87–98.

[4] M. A. Bhat, *Energy of weighted digraphs*, Discrete Applied Mathematics **223** (2017), 1–14.

[5] C. Champagne, D. G. Salthouse, R. Paul, V.-M. Cao-Lormeau, B. Roche, B. Cazelles, *Structure in the variability of the basic reproductive number (R_0) for Zika epidemics in the Pacific Islands*, eLife **5** (2016), e19874.

[6] G. Chartrand, P. Zhang, *Introduction to Graph Theory*, McGraw-Hill, New York, 2004.

[7] N. Chitnis, J. M. Cushing, J. M. Hyman, *Bifurcation analysis of a mathematical model for malaria transmission*, SIAM Journal on Applied Mathematics **67** (2006), 24–45.

[8] N. M. Ferguson, Z. M. Cucunubá, I. Dorigatti, et al., *Countering the Zika epidemic in Latin America*, Science **353** (2016), 353–354.

[9] I. Gutman, *The energy of a graph*, Berichte der Mathematisch-Statistischen Sektion im Forschungszentrum Graz **103** (1978), 1–22.

[10] S. Hafeez, M. Khan, *Iota energy of weighted digraphs*, Transactions on Combinatorics **7** (2018), 55–73.

[11] J. M. Heffernan, R. J. Smith, L. M. Wahl, *Perspectives on the basic reproductive ratio*, Journal of the Royal Society Interface **2** (2005), 281–293.

[12] H. W. Hethcote, *The mathematics of infectious diseases*, SIAM Review **42** (2000), 599–653.

[13] Y. Jiang, *Study on eigenvalue and eigenvector introduction*, Journal of Physics: Conference Series **2282** (2022), 012004.

[14] M. Khan, R. Farooq, J. Rada, *Complex adjacency matrix and energy of digraphs*, Linear and Multilinear Algebra **65** (2017), 2170–2186.

[15] C. A. Manore, K. S. Hickmann, S. Xu, H. J. Wearing, J. M. Hyman, *Comparing dengue and chikungunya emergence and endemic transmission in Aedes aegypti and Aedes albopictus*, Journal of Theoretical Biology **356** (2014), 174–191.

[16] A. Momoh, A. Fügenschuh, *Optimal control of intervention strategies and cost effectiveness analysis for a Zika virus model*, Operations Research for Health Care **18** (2018), 99–111.

[17] S. C. Mpeshe, N. Nyerere, S. Sanga, *Modeling approach to investigate the dynamics of Zika virus fever: a neglected disease in Africa*, International Journal of Advances in Applied Mathematics and Mechanics **4** (2017), 14–21.

[18] P. Suparit, A. Wiratsudakul, C. Modchang, *A mathematical model for Zika virus transmission dynamics with a time-dependent mosquito biting rate*, Theoretical Biology and Medical Modelling **15** (2018), 11.